

Zero magnetization in a disordered $(\text{La}_{1-x/2}\text{Bi}_{x/2})(\text{Fe}_{0.5}\text{Cr}_{0.5})\text{O}_3$ uncompensated weak ferromagnet

This article has been downloaded from IOPscience. Please scroll down to see the full text article.

2009 J. Phys.: Condens. Matter 21 486002

(<http://iopscience.iop.org/0953-8984/21/48/486002>)

View [the table of contents for this issue](#), or go to the [journal homepage](#) for more

Download details:

IP Address: 129.252.86.83

The article was downloaded on 30/05/2010 at 06:17

Please note that [terms and conditions apply](#).

Zero magnetization in a disordered $(\text{La}_{1-x/2}\text{Bi}_{x/2})(\text{Fe}_{0.5}\text{Cr}_{0.5})\text{O}_3$ uncompensated weak ferromagnet

K Vijayanandhini¹, Ch Simon¹, V Pralong¹, Y Bréard¹,
V Caignaert¹, B Raveau¹, P Mandal², A Sundaresan² and
C N R Rao²

¹ CRISMAT, UMR 6508, CNRS-ENSICAEN, Université de Caen, 14050 Caen, France

² Jawaharlal Nehru Center for Advanced Scientific Research, Jakkur PO, Bangalore 560064, India

E-mail: bernard.raveau@ensicaen.fr

Received 15 July 2009, in final form 8 October 2009

Published 30 October 2009

Online at stacks.iop.org/JPhysCM/21/486002

Abstract

The orthorhombic perovskite, $(\text{La}_{1-x/2}\text{Bi}_{x/2})(\text{Fe}_{0.5}\text{Cr}_{0.5})\text{O}_3$ was investigated for $0 \leq x \leq 1$. Its space group, $Pnma$, compatible with the disordering of iron and chromium in the B sites, confirms previous observations. More importantly this compound is found to be an uncompensated weak ferromagnet, with a very peculiar zero magnetization behaviour, generally observed for ordered magnetic cations in the B sites. It exhibits a magnetic transition at high temperature (T_C) above 450 K, while the zero magnetization occurs between 100 and 160 K depending on the x -value. The AC magnetic susceptibility study shows that this compound does not exhibit a spin glass or cluster glass behaviour, in contrast to what was suggested for the $x = 0$ compound. This zero magnetization phenomenon can be interpreted by the fact that this perovskite is an uncompensated weak ferromagnet, which consists of canted weak ferromagnetic domains and clusters of pure chromium and pure iron composition, antiferromagnetically coupled through Cr–O–Fe interactions.

(Some figures in this article are in colour only in the electronic version)

1. Introduction

The phenomenon of zero magnetization was discovered several decades ago in spinel compound [1] after the prediction by Néel [2], that in a ferrimagnetic material consisting of two or more types of antiferromagnetically ordered magnetic ions, the magnetic moment can vary in such a way that the magnetization reverses and crosses zero at a temperature (in response to a small applied magnetic field) called the compensation temperature, T_{comp} . Such a phenomenon is rare and is related to the fact that the magnetocrystalline anisotropy is strong enough to prevent the flipping of the spins to align with the applied magnetic field.

The temperature induced magnetization reversal was then observed in a very limited number of systems including (i) LaVO_3 [3], (ii) Pd–Fe alloys [4], (iii) $\text{Gd}_{1-x}\text{Ca}_x\text{MnO}_3$ manganites [5], $\text{La}_{1-x}\text{Pr}_x\text{CrO}_3$ [6] and GdCrO_3 [7], (iv)

YbFe_4Al_8 [8] and (v) $\text{Sm}_{1-x}\text{Gd}_x\text{Al}_2$ [9]. In the V(III) oxides, LaVO_3 , the tilting of magnetically inequivalent, V^{3+} sites during the cooperative first order magnetostrictive distortion is associated with an abrupt change in both spin and orbital ordering and hence induces the magnetization reversal [10]. In chromium oxides, GdCrO_3 or $\text{La}_{1-x}\text{Pr}_x\text{CrO}_3$, the magnetization reversal was understood in connection with the opposite direction of the rare-earth paramagnetic spins (Gd^{3+} or Pr^{3+}) to that of the canted antiferromagnetic (AFM) spins of Cr^{3+} . In this case, the AFM interaction between the cations from both A- and B-sublattices are involved. For Pd–Fe alloys [4], the magnetization reversal is ascribed to the inhomogeneous distribution of magnetic flux within the sample. Recently a zero magnetization was discovered in (111) $\text{Sm}_{1-x}\text{Gd}_x\text{Al}_2$ epitaxial films [9]. These compounds present a compensation temperature, T_{comp} , at which a long range ferromagnetic order persists while the net magnetization

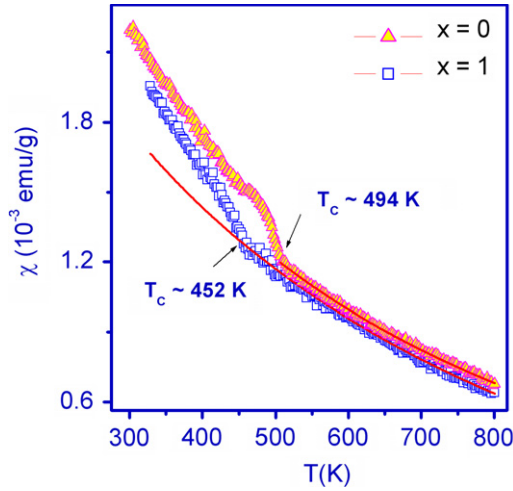


Figure 1. Susceptibility (χ) as a function of temperature, measured under $H = 0.3$ T for $(\text{La}_{1-x/2}\text{Bi}_{x/2})(\text{Fe}_{0.5}\text{Cr}_{0.5})\text{O}_3$ with $x = 0$ and 1. The open symbols and solid lines represent the experimental data and Curie–Weiss fit in the high temperature paramagnetic region.

is zero. The authors have shown that at T_{comp} , a perfect cancellation of the antiparallel coupled orbital moment (L) of Sm^{3+} and the total spin moments (S) of Sm^{3+} and Gd^{3+}

(the orbital moment of Gd^{3+} is zero) leads to the zero magnetization. However, x-ray magnetic circular dichroism at Sm and Gd $L_{2,3}$ edges attested the evidence of long range magnetic ordering of Sm and Gd sublattices at T_{comp} , and a parallel coupling between the total magnetic moment of Sm^{3+} and Gd^{3+} [9].

Recently, the nuclear and magnetic structure of $\text{LaFe}_{0.5}\text{Cr}_{0.5}\text{O}_3$ was investigated by neutron and electron diffraction [11]. It was shown that $\text{LaFe}_{0.5}\text{Cr}_{0.5}\text{O}_3$ exhibits a perovskite structure in which Fe^{3+} and Cr^{3+} are randomly positioned at B site having an antiferromagnetic ordering with a Neel temperature of 265 K. The magnetic structure of $\text{LaFe}_{0.5}\text{Cr}_{0.5}\text{O}_3$ was studied and the results showed the coexistence of zero magnetization effect within the antiferromagnetic ordered sublattices. Further, the authors in [11] have attributed the uncompensated weak magnetic moments to a magnetic cluster state which holds up to 550 K, but they did not show special interest for the zero magnetization effect, in this system, despite the fact that the report was mainly focused on magnetic structural determination. Moreover, since the two magnetic cations, Fe^{3+} and Cr^{3+} , occupy the same site and are disordered, it was not possible to refine the respective magnetic moments of the two different cations and only the averaged value was found, suggesting an antiferromagnetic structure.

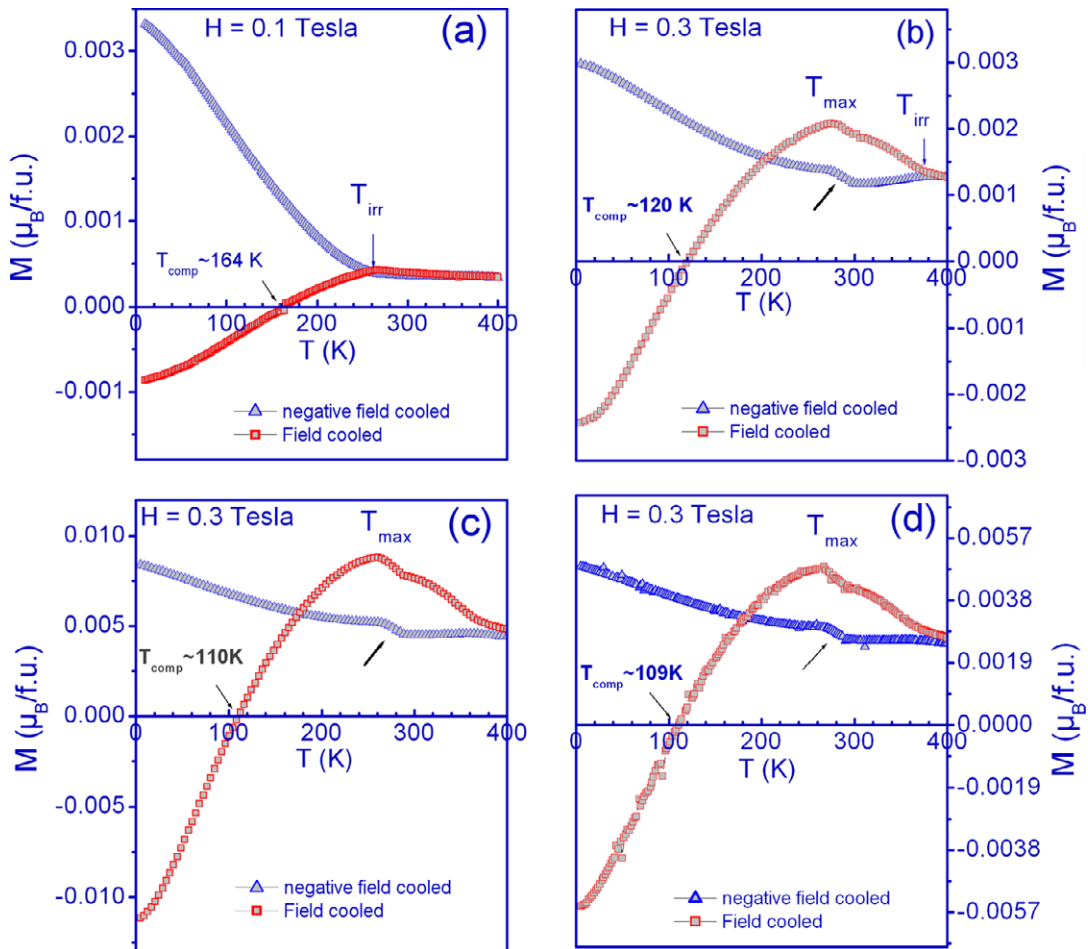


Figure 2. The magnetization versus temperature $M(T)$ measured under field cooled FC(C) and negative field cooled FC(N) modes at applied magnetic fields (H) of 0.3 T for $(\text{La}_{1-x/2}\text{Bi}_{x/2})(\text{Fe}_{0.5}\text{Cr}_{0.5})\text{O}_3$ with (a) $x = 0$, (b) $x = 0.25$, (c) $x = 0.5$ and (d) $x = 1$.

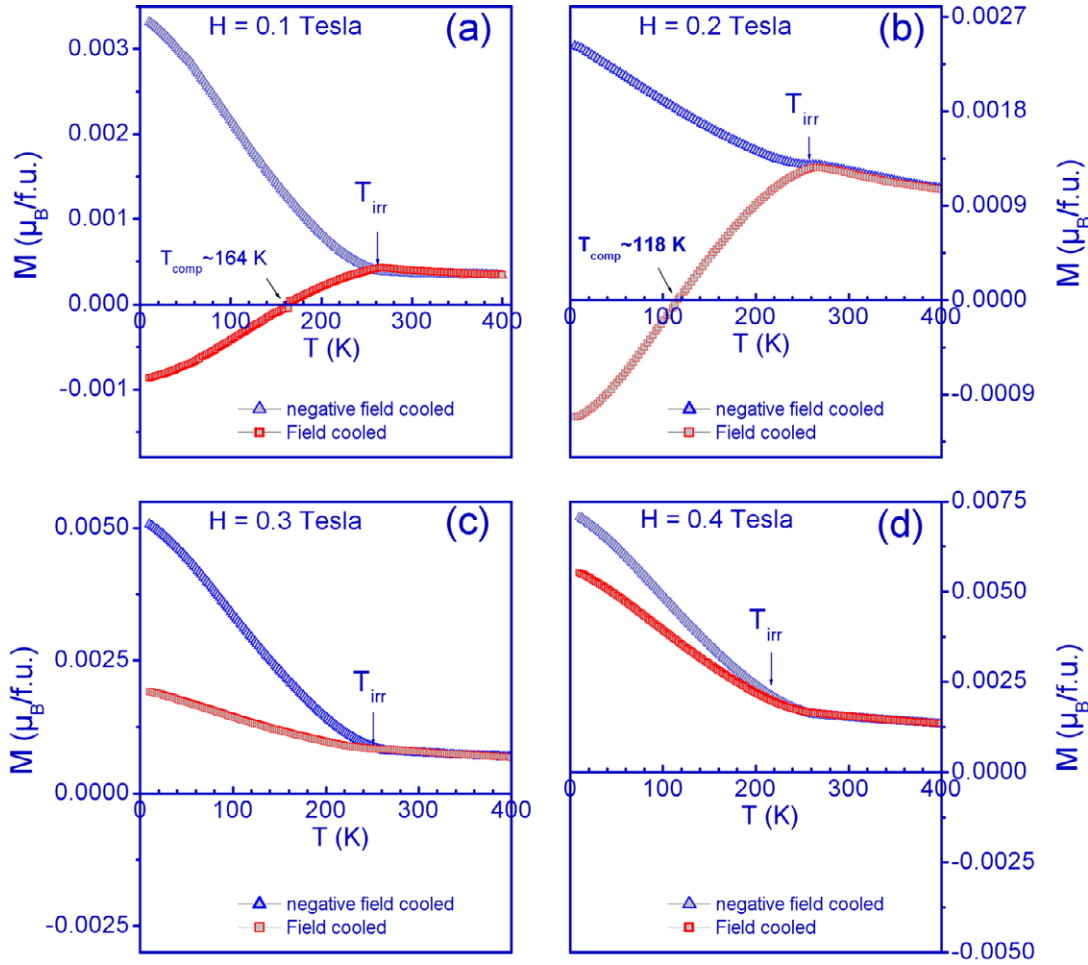


Figure 3. The magnetization versus temperature $M(T)$ for $\text{LaFe}_{0.5}\text{Cr}_{0.5}\text{O}_3$ ($x = 0$), measured at various applied magnetic fields (H): (a) 0.1 T, (b) 0.2 T, (c) 0.3 T and (d) 0.4 T.

In the present paper, we will show that, differently from the published neutron scattering study by Azad *et al* [11], $\text{LaFe}_{0.5}\text{Cr}_{0.5}\text{O}_3$ is an uncompensated weak ferromagnet, with a zero magnetization phenomenon. This revises the magnetism of the compound completely. Further, we report the existence of a temperature dependent magnetization reversal phenomena for a series of compounds, $(\text{La}_{1-x/2}\text{Bi}_{x/2})(\text{Fe}_{0.5}\text{Cr}_{0.5})\text{O}_3$ with $0 \leq x \leq 1$, whose compensation temperature (T_{comp}) could be extended by varying the bismuth content.

2. Experimental details

Phase-pure polycrystalline samples of $(\text{La}_{1-x/2}\text{Bi}_{x/2})(\text{Fe}_{0.5}\text{Cr}_{0.5})\text{O}_3$ with $0 \leq x \leq 1$ were prepared by solid state reaction technique by mixing stoichiometric quantities of La_2O_3 (99.96%, Fluka), Bi_2O_3 (99.98%), Cr_2O_3 (99.96%), and Fe_2O_3 (99.98%) (all chemicals from Merck) and subsequent heat treatment at 873 K (12 h) in air. The powders were ground again and further calcined at ~ 1173 K (48 h). The granulated powder was then pressed into rectangular bars under 200 MPa, sintered at $T_{\text{sinter}} \sim 1273$ K (24 h) and cooled at a rate of 120°C h^{-1} . The sintered ceramics bars were post-sinter annealed in air for extended periods of 30–48 h at $T_{\text{anneal}} <$

T_{sinter} in order to improve the oxygen homogeneity. The phase purity of $(\text{La}_{1-x/2}\text{Bi}_{x/2})(\text{Fe}_{0.5}\text{Cr}_{0.5})\text{O}_3$ was ascertained by x-ray powder diffraction (XRPD). The chemical analysis of the sample using iodometric titration shows that the oxygen stoichiometry is ' $\text{O}_{3.01 \pm 0.01}$ '. The energy dispersive x-ray analyses (EDX), along with the scanning electron microscopy (SEM) of the thermally etched surfaces of $(\text{La}_{1-x/2}\text{Bi}_{x/2})(\text{Fe}_{0.5}\text{Cr}_{0.5})\text{O}_3$ samples at the grain interiors, as well as the intergrain regions, confirm that the cation ratios are in good agreement with the nominal one and are within the limit of the experimental errors. The specimens did not show any discernible secondary phases either from the EDX of the cross-sectional samples or from SEM studies under high magnification in the backscattering mode. Mössbauer spectroscopy has also been performed, showing that iron is trivalent for the studied compounds. The x-ray powder diffraction (XRPD) pattern was registered with a Panalytical X'Pert Pro diffractometer having a nickel filtered $\text{Cu K}\alpha$ source under a continuous scanning method in the 2θ range of 5° – 120° with a step size of $\Delta 2\theta = 0.0167^\circ$. A Rietveld analysis of XRPD data was carried out with the FULLPROF refinement program [12]. The dc magnetization (DCM) measurements were performed using a superconducting quantum interference device magnetometer

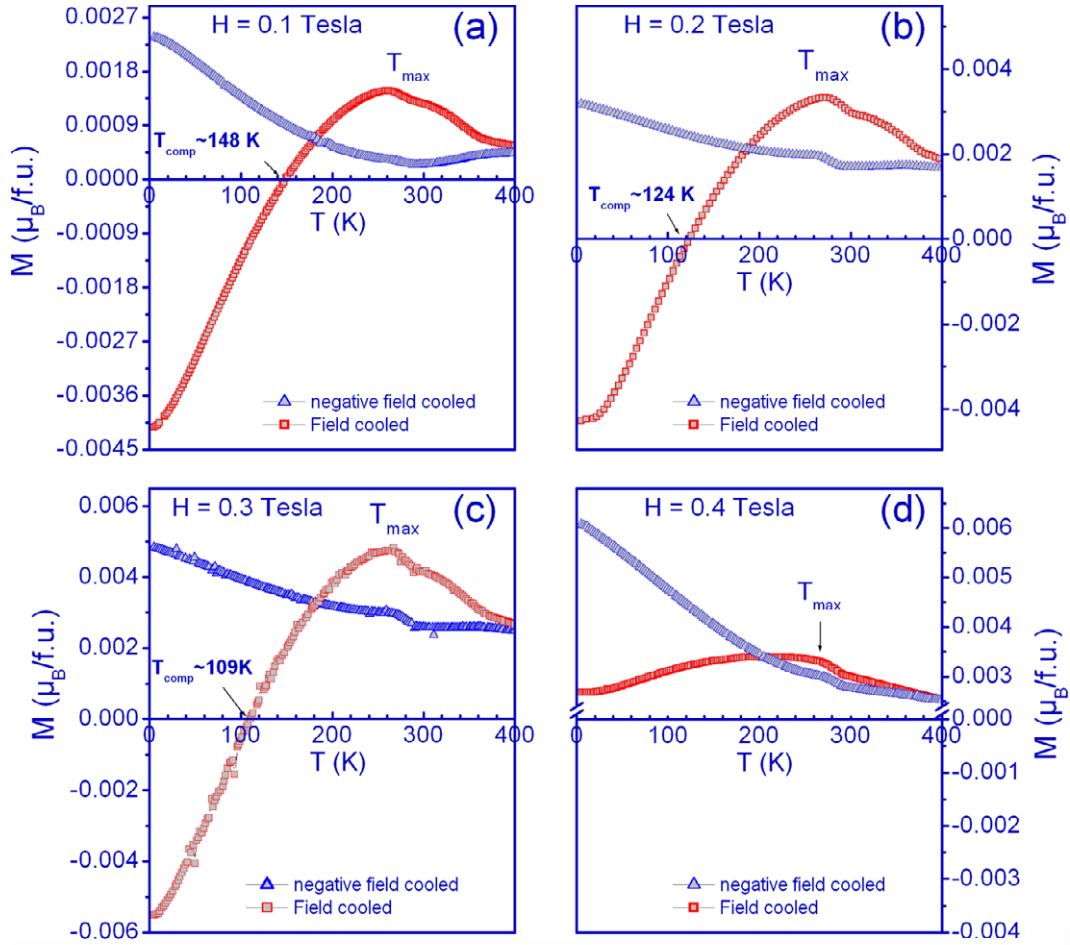


Figure 4. The magnetization versus temperature $M(T)$ for $(La_{0.5}Bi_{0.5})(Fe_{0.5}Cr_{0.5})O_3$ with $x = 1$ measured at various applied magnetic fields (H): (a) 0.1 T, (b) 0.2 T, (c) 0.3 T and (d) 0.4 T.

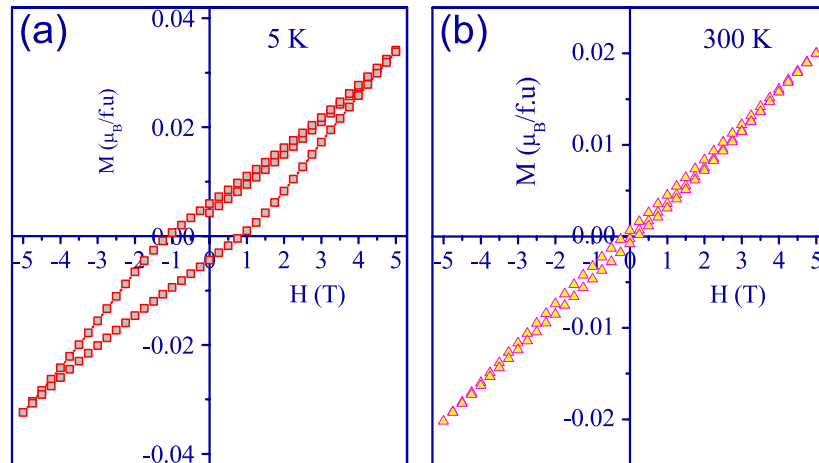


Figure 5. Magnetization (M) as a function of field (H) for $(La_{0.5}Bi_{0.5})(Fe_{0.5}Cr_{0.5})O_3$ ($x = 1$) measured at (a) 5 K and (b) 300 K.

(SQUID) equipped with variable temperature cryostat (Quantum Design, San Diego, USA) (1.8–400 K, 0–5 T). The ac susceptibility, $\chi_{ac}(T)$, was measured with a physical property measurement system from Quantum Design (PPMS) with the frequency ranging from 125 to 10 kHz, between 5 and 320 K ($H_{dc} = 0$ Oe and $H_{ac} = 10$ Oe).

3. Results and discussion

The XRPD patterns of $(La_{1-x/2}Bi_{x/2})(Fe_{0.5}Cr_{0.5})O_3$ with ($0 \leq x \leq 1$) registered at four different temperature –100, 170, 220 and 300 K—could be indexed to an orthorhombic cell, space group $Pnma$ (table 1). No detectable secondary phases, even

Table 1. Crystallographic data at room temperature for $(\text{La}_{1-x/2}\text{Bi}_{x/2})(\text{Fe}_{0.5}\text{Cr}_{0.5})\text{O}_3$ with $x = 0$ and 1.

Compound	$\text{LaFe}_{0.5}\text{Cr}_{0.5}\text{O}_3$	$\text{La}_{0.5}\text{Bi}_{0.5}\text{Fe}_{0.5}\text{Cr}_{0.5}\text{O}_3$
Formula weight	240.83 g mol ⁻¹	275.87 g mol ⁻¹
Crystal system	Orthorhombic	Orthorhombic
Space group	<i>Pnma</i> (62)	<i>Pnma</i> (62)
Cell parameters	$a = 5.5242(0)$ Å $b = 7.8114(1)$ Å $c = 5.5397(0)$ Å	$a = 5.5393(1)$ Å $b = 7.8171(1)$ Å $c = 5.5246(1)$ Å
Cell volume	239.05(3) Å ³	239.22(1) Å ³
Calc. density	3.35 g cm ⁻³	3.83 g cm ⁻³
χ^2	4.88	4.53
R_B	5.4%	7.9%

Table 2a. Fractional atomic coordinates for $(\text{La}_{1-x/2}\text{Bi}_{x/2})(\text{Fe}_{0.5}\text{Cr}_{0.5})\text{O}_3$ with $x = 1$.

Atom	Wyck.	x/a	y/b	z/c
La	4c	0.0273(4)	1/4	0.9941(14)
Bi	4c	0.0273(4)	1/4	0.9941(14)
Fe	4b	0	0	1/2
Cr	4b	0	0	1/2
O1	4c	0.499(6)	1/4	0.053(12)
O2	8d	0.265(10)	0.052(5)	0.716(9)

Table 2b. Fractional atomic coordinates for $(\text{La}_{1-x/2}\text{Bi}_{x/2})(\text{Fe}_{0.5}\text{Cr}_{0.5})\text{O}_3$ with $x = 0$.

Atom	Wyck.	x/a	y/b	z/c
La	4c	0.0241(3)	1/4	0.9959(13)
Fe	4b	0	0	1/2
Cr	4b	0	0	1/2
O1	4c	0.493(4)	1/4	0.065(6)
O2	8d	0.266(6)	0.046(4)	0.731(6)

as minor reflections in the XRPD patterns, were discernible for the studied specimens. Structure refinements of the $x = 1$ sample led to reliability factors (R) and goodness-of-fit (χ^2) indicators up to $\sim 7.9\%$ and ~ 4.53 respectively. The crystallographic data are listed in tables 2a and 2b. They are in agreement with previous neutron diffraction data [11], which did not show any sign of ordering between Fe^{3+} and Cr^{3+} cations. Note that the specimens do not show any kind of structural or crystal symmetry change versus temperature in the range 100–300 K.

The susceptibility versus temperature, $\chi_{\text{dc}}(T)$ curves measured between 300 and 800 K for $(\text{La}_{1-x/2}\text{Bi}_{x/2})(\text{Fe}_{0.5}\text{Cr}_{0.5})\text{O}_3$ specimens indicate a ferrimagnetic (FiM) or weak ferromagnetic (WFM) to paramagnetic (PM) transition (T_C) at high temperature above 400 K (figure 1). The FiM (or WFM) to PM ordering temperature, T_C , shifts to lower values with Bi-substitution. For $x = 0$, the FiM (or WFM) to PM transition was observed at $T_C \sim 494$ K, whereas, for $x = 1$, the T_C decreases to ~ 452 K (table 3). The T_C value could be shifted between 452 and 494 K, by varying the Bi-substitution (x value) at the La site in $(\text{La}_{1-x/2}\text{Bi}_{x/2})(\text{Fe}_{0.5}\text{Cr}_{0.5})\text{O}_3$ and hence crucially depends on La/Bi ratio. Above T_C , the susceptibility, $\chi_{\text{dc}}(T)$ data, fitted with Curie–Weiss law, $\chi = C/(T - \theta_{\text{CW}})$, evidences a large negative Curie–Weiss temperature

Table 3. The magnetic properties of $(\text{La}_{1-x/2}\text{Bi}_{x/2})(\text{Fe}_{0.5}\text{Cr}_{0.5})\text{O}_3$ with $x = 0$ and 1 samples obtained from the DC magnetization data. The effective paramagnetic moment μ_{eff} was calculated in the paramagnetic regime of high temperature susceptibility data.

Magnetic parameters	$\text{LaFe}_{0.5}\text{Cr}_{0.5}\text{O}_3$	$\text{La}_{0.5}\text{Bi}_{0.5}\text{Fe}_{0.5}\text{Cr}_{0.5}\text{O}_3$
Curie temperature, T_C	494 K	452 K
Curie–Weiss temperature, θ_{CW}	–292 K	–529 K
Compensation temperature, T_{comp} ($H \sim 0.1$ T)	164 K	148 K
Effective paramagnetic moment, μ_{eff}	2.63 $\mu_B/\text{f.u.}$	3.51 $\mu_B/\text{f.u.}$
Coercivity at 5 K, $H_{c,5\text{K}}$	0.55 T	0.96 T

($\theta_{\text{CW}} = -292$ K, for $x = 0$) and Curie constant of 2.12 emu K/Oe.g. The large negative θ_{CW} values indicate strong AFM coupling. The effective magnetic moment (μ_{eff}) calculated from the linear region of $\chi_{\text{dc}}(T)$ curve is $\sim 2.63 \mu_B/\text{f.u.}$ (for $x = 0$), which is lower than the expected value for $\text{Fe}^{3+}/\text{Cr}^{3+}$ high spin configuration ($\mu_{\text{eff}} = 3.9$ – $4.9 \mu_B$) (table 3). The observation of a ferro (ferri) magnetic order at high temperature seems to be in contradiction with Azad *et al* [11], who claim that the compound is antiferromagnetic (AFM) with $T_N = 265$ K. But, in fact they observe by neutron diffraction a diffuse magnetic reflection up to 500 K. It should be noted that Belayachi *et al* [13] also observed a magnetic transition at 450 K from susceptibility measurements, while Mössbauer spectroscopy (this work and [13]) indicates that iron is in a paramagnetic state at room temperature.

The DC magnetization studies of $(\text{La}_{1-x/2}\text{Bi}_{x/2})(\text{Fe}_{0.5}\text{Cr}_{0.5})\text{O}_3$ with $x = 0, 0.25, 0.5, 1$ show zero magnetization phenomena (figures 2(a)–(d)). In order to induce this effect, the $M(T)$ curves were registered both during the warming after cooling under magnetic field (H) of ~ 0.3 T (field cooled, FC mode) and also during warming under the field (H) of ~ 0.3 T after reversing the magnetization by the application of -0.3 T (negative field cooled, NFC mode). For $x = 0$, the M_{FC} and M_{NFC} curves merge with each other between 400 and 258 K and show a nearly constant magnetization value of $\sim 0.0003 \mu_B/\text{f.u.}$ (figure 2(a)). Below $T_{\text{irr}} \sim 258$ K, the M_{FC} and M_{NFC} curves exhibit a strong irreversibility, as indicated by the appearance of a large bifurcation between them. Moreover, on cooling below the irreversibility temperature, T_{irr} , the $M_{\text{FC}}(T)$ curve decreases and crosses a zero value at the compensation temperature, $T_{\text{comp}} \sim 164$ K. The curve further decreases down to a minimum magnetization value of $\sim -0.0008 \mu_B/\text{f.u.}$ at ~ 5 K. Due to the zero magnetization effect, the $M_{\text{FC}}(T)$ and $M_{\text{NFC}}(T)$ curves significantly deviate from each other from $T_{\text{irr}} \sim 258$ K (for $x = 0$), beyond which the polarity of the magnetization is negative. The $M_{\text{FC}}(T)$ curves continue to monotonically decrease with cooling until 5 K. Therefore, the M_{FC} curves are located far below the $M_{\text{NFC}}(T)$ curves, as demonstrated for the $x = 0$ sample at $H \sim 0.1$ T (figure 2(a)). Such a negative magnetization phenomena (reversal of magnetization) is not a normal behaviour of magnetic materials. The negative magnetization (at T_{comp})

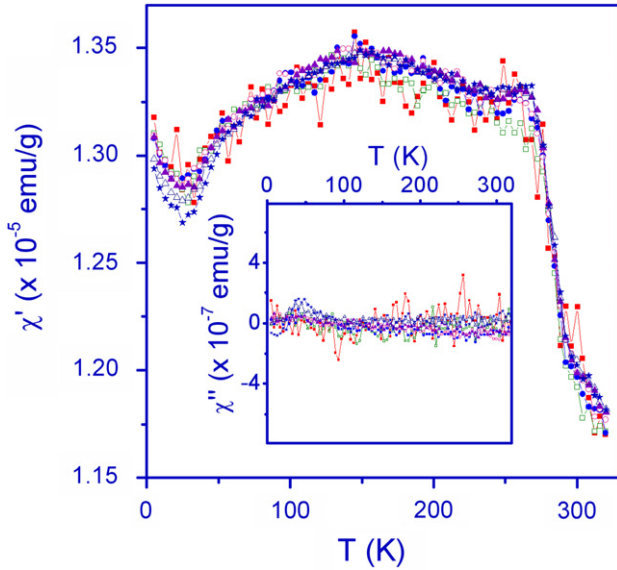


Figure 6. The real (in-phase) χ' component of ac susceptibilities for $(\text{La}_{0.5}\text{Bi}_{0.5})(\text{Fe}_{0.5}\text{Cr}_{0.5})\text{O}_3$ ($x = 1$), as a function of temperature at the frequency $f = 125$ Hz–10 kHz at zero static magnetic field (H_{dc}), and at a driving ac fields (H_{ac}) of 10 Oe. The measuring frequencies (in Hz) are: 125 (■), 325 (□), 525 (●), 725 (○), 1000 (▲), 5000 (△) and 10000 (*). Inset: The imaginary (out-of-phase) χ'' component of ac susceptibilities for the same sample.

implies that the direction of effective magnetization of the specimen is exactly opposite to that of the applied magnetic field.

With Bi-substitution in $(\text{La}_{1-x/2}\text{Bi}_{x/2})(\text{Fe}_{0.5}\text{Cr}_{0.5})\text{O}_3$ ($x = 0.25$ –1), the samples show a step like magnetic anomaly (indicated by arrows) in the $M_{\text{FC}}(T)$ and $M_{\text{NFC}}(T)$ curves at around 280 K (figures 2(b)–(d)). On cooling the samples in FC mode, the $M_{\text{FC}}(T)$ curve exhibits a broad magnetization peak at T_{max} showing an irreversible hysteresis between M_{FC} and M_{NFC} up to 400 K. Since 400 K is the maximum temperature of the experimental set up, it is not possible to determine T_{irr} for $x > 0.25$ samples, which can be any value between 400 K and T_{C} . The magnetization shows a maximum value (M_{max}) with a positive polarity at the peak temperature, T_{max} , between ~ 274.2 K ($x = 0.25$) (figure 2(b)) and ~ 258.5 K ($x = 1$) (figure 2(d)), which decreases with the Bi-substitution. On further cooling down, it leads to the magnetization reversal at $T_{\text{comp}} \sim 120$ K for $x = 0.25$ (figure 2(b)). Further, the compensation temperature decreases with Bi-substitution to ~ 110 K for $x = 0.5$ and to ~ 109 K for $x = 1$ (figures 2(c) and(d)). However, for all Bi-substituted samples, the absolute value of minimum magnetization (M_{min} at 5 K) is close to that of M_{max} . The negative magnetization appears for a wide compositional range of $0 \leq x \leq 1$, wherein, the T_{comp} decreases with increasing Bi-content.

On increasing the applied magnetic field H , the absolute value of negative magnetization in the $M_{\text{FC}}(T)$ curve decreases monotonically for $\text{LaFe}_{0.5}\text{Cr}_{0.5}\text{O}_3$ (figures 3(a)–(d)). Further, there is a shift in the compensation temperatures (T_{comp}) to lower values from 164 K ($H = 0.1$ T) to 118 K ($H = 0.2$ T) with increasing external magnetic field (H) (figures 3(a)

and (b)). However, there exists a threshold magnetic field above which no negative magnetization in M_{FC} curve is observed in the measured temperature range of 5–400 K i.e., the M_{FC} shift to positive values for applied magnetic field H between 0.2 and 0.3 T (figures 3(b)–(d)). Qualitatively, an identical magnetic field dependent shift in T_{comp} has been observed for all the $(\text{La}_{1-x/2}\text{Bi}_{x/2})(\text{Fe}_{0.5}\text{Cr}_{0.5})\text{O}_3$ samples with $0 \leq x \leq 1$, wherein the threshold value of the applied field at which the negative magnetization in $M_{\text{FC}}(T)$ completely shifts to a positive value is different for each composition. This is further demonstrated for the $x = 1$ sample in figures 4(a)–(d), wherein the threshold magnetic field (H) value is between 0.3 and 0.4 T, below which the sample can exhibit the negative magnetization phenomena associated with a shift in T_{comp} under the applied magnetic field (figures 4(c)–(d)).

In order to check the ferri- or ferromagnetic nature of $(\text{La}_{1-x/2}\text{Bi}_{x/2})(\text{Fe}_{0.5}\text{Cr}_{0.5})\text{O}_3$, we have measured the isothermal field driven dc magnetization $M(H)$ curves at different temperatures (figures 5(a) and (b)). The $M(H)$ curves for the sample with $x = 1$, show a large hysteresis loop at 5 K with a remnant magnetization (M_{r}) value of $0.005 \mu_{\text{B}}/\text{f.u.}$ and a coercive field (H_{c}) of ~ 0.96 T (figure 5(a)), whose value is much larger than the magnetic field used for DC magnetization (M_{FC} and M_{NFC}) measurements (figure 2). Then, above 5 K, coercive fields (H_{c} 's) decreases rapidly, to ~ 0.27 T at 100 K and to ~ 0.18 T at 300 K (figure 5(b)) and finally above T_{C} , the $M(H)$ behaviour becomes linear, indicative of the paramagnetic behaviour at high temperature. The $M(H)$ curves below the magnetic transition (T_{C}) clearly show a lack of magnetic saturation even under the magnetic field of 5 T. The highest saturation magnetization (μ_{H}) obtained at 5 K is $0.009 \mu_{\text{B}}/\text{f.u.}$ The μ_{H} values were determined at the ordinate point intercepted by the extrapolation from the linear high-field region of $M(H)$ curve. The low value of the experimental magnetic moment at 5 T ($\sim 0.03 \mu_{\text{B}}/\text{f.u.}$ for $x = 1$) shows that this phenomenon does not originate from a ferrimagnetic coupling between Fe^{3+} ($e_{\text{g}}^2 t_{2\text{g}}^3$; $M_0 = 5 \mu_{\text{B}}$) and Cr^{3+} ($e_{\text{g}}^0 t_{2\text{g}}^3$; $M_0 = 3 \mu_{\text{B}}$) sublattices, which would lead to saturation magnetization $M_0 = 5 \mu_{\text{B}} - 3 \mu_{\text{B}} = 2 \mu_{\text{B}}$. However, it is clear that the negative magnetization could not be due to conventional diamagnetism, since the differential magnetic susceptibility (dM/dH) is positive throughout the measured field range (figure 2).

In order to test the possible presence of magnetically frustrated spin behaviour, the dynamic magnetic properties were studied by way of ac magnetic susceptibility measurements for these specimens (figure 6). The real part (in-phase) component of the ac magnetic susceptibility $\chi'_{\text{ac}}(T, f)$ curves, were registered at zero dc magnetic field ($H_{\text{dc}} = 0$) between 5 and 320 K and with the frequency (f) ranging from 10 Hz to 10 kHz, using the PPMS. The amplitude of the ac magnetic field was $H_{\text{ac}} \sim 10$ Oe. The $\chi'_{\text{ac}}(T)$ curves do not show any frequency dependency measured up to 3 decades down to 5 K. However, the $\chi'_{\text{ac}}(T)$ curves of the bismuth substituted compounds are different from the pure La phase. One observes a steep increase in the χ'_{ac} values around ~ 280 K, at the temperature where a small step like magnetic anomaly is seen in the DC magnetization, $M(T)$ curves (figure 5). However,

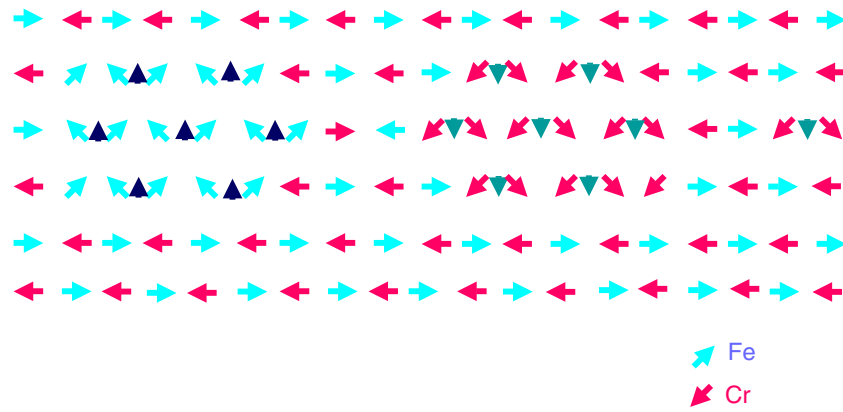


Figure 7. Schematized representation of weak ferromagnetic Fe_n and Cr_n domains or clusters distributed at random and antiferromagnetically coupled in the perovskite matrix.

the imaginary component (out-of-phase) of ac susceptibility, χ''_{ac} , does not exhibit any peak corresponding to magnetic relaxation or energy losses at the compensation temperature, T_{comp} (inset in figure 6). Hence, in contrast to the report by Azad *et al* [11], the $(La_{1-x/2}Bi_{x/2})(Fe_{0.5}Cr_{0.5})O_3$ series of compounds do not show any signature related to spin glass.

In the present compounds, where the Fe^{3+} and Cr^{3+} species are distributed in a disordered way in the B sublattice, the model of compensation of orbital magnetic moments (L) and total spin moments (S) as proposed by Avisou *et al* [9] is rather unlikely since the expected orbital moment is too small to compensate the Fe^{3+} and Cr^{3+} spin moments. Similarly, the model proposed by Néel [2] for zero magnetization, which would require a 1:1 ordering of Fe^{3+} and Cr^{3+} species cannot apply. More importantly, the fact that this phenomenon would originate from local 1:1 ordered ‘Fe, Cr’ ferrimagnetic regions is not believable, due to the high difference between the magnetic moments of Fe^{3+} ($S = 5/2$) and Cr^{3+} ($S = 3/2$). The latter implies that a much higher magnetic field would be required to reverse these moments and reach zero magnetization and does not explain the variation of the magnetization versus temperature.

At this point, we have to consider the three types of magnetic interactions that take place in this perovskite framework, corresponding to the Cr–O–Cr, Fe–O–Fe and Cr–O–Fe bonds respectively. According to Kanamori–Goodenough (KG) rules [14], the Fe–O–Fe and Cr–O–Cr superexchange interactions are antiferromagnetic, while Cr–O–Fe is predicted to be ferromagnetic. But the sign of this last interaction (Cr–O–Fe) is not firmly established. Recent band-structure calculations predict either an antiferromagnetic interaction between Fe^{3+} and Cr^{3+} for double ordered perovskites [15], or a ferromagnetic coupling [16]. Ueda *et al* [17] reported ferromagnetic Cr–O–Fe interactions in thin films of ordered superlattices $LaFeO_3$ – $LaCrO_3$. Nevertheless the experimental magnetic behaviour is always antiferromagnetic for bulk samples with a disordered Fe–Cr lattice [11, 13, 17]. Thus, we can consider that the matrix of these perovskites should be antiferromagnetic. However, we must keep in mind that both perovskites, $LaFeO_3$ [18] and $LaCrO_3$ [19], are in fact weak ferromagnets (WFM) due to spin canting.

Consequently, the phenomenological model first proposed by Tamine *et al* for $Fe_{0.66}Cr_{0.33}F_3$ [20] can be applied here. It is indeed most probable that the observed properties result from the existence of two types of uncompensated weak ferromagnetic Cr_n and Fe_n domains and clusters that are distributed at random in the AFM $(Cr_1Fe_1)_n$ matrix, and are antiferromagnetically coupled as schematized on figure 7. As a consequence, the transverse magnetic components of the Cr_n and Fe_n domains are oriented in opposite directions, leading to a ferrimagnetic-like behaviour due to dipolar interaction. When the magnetic field is applied parallel to these two transverse ferromagnetic components, one of them will be aligned parallel to the field and the second one will be aligned antiparallel. Thus by increasing the magnetic field, the antiparallel component can be switched in the field direction, for a critical value of the field. Similarly, the two small ferromagnetic transverse components, for Cr and Fe respectively, strongly depend on temperature, and have different ordering temperature, so that there exists a temperature, called the temperature of compensation, where the parallel and antiparallel transverse components compensate each other. A similar model was proposed previously for the perovskites of the system $LaFe_{1-x}Cr_xO_3$ [13], but the authors did not find any clear evidence of a compensation point of the magnetization.

4. Conclusions

In conclusion, we have observed an unusual zero magnetization phenomenon in $(La_{1-x/2}Bi_{x/2})(Fe_{0.5}Cr_{0.5})O_3$ at a compensation temperature under an applied external magnetic field. It is remarkable that this zero magnetization phenomenon does not originate from a ferrimagnetic ordering of the Fe^{3+} and Cr^{3+} cations, but is due to the canting of pure ‘ $La_{1-x}Bi_xFeO_3$ ’ and ‘ $La_{1-x}Bi_xCrO_3$ ’ domains or clusters, that are coupled antiferromagnetically. Another aspect is that these zero magnetic moment uncompensated weak ferromagnets have high magnetic ordering temperatures with $T_C > 450$ K, as compared to the so far reported compounds and also exhibit an extendable compensation temperature with respect

to composition (x). These results suggest that similar uncompensated weak ferromagnets involving a zero magnetization effect should exist, for different pairs of magnetic cations and that the 1:1 Fe:Cr composition may not be a necessary condition for the appearance of this phenomenon.

References

- [1] Gorter E W and Schulkes J A 1953 *Phys. Rev.* **89** 487
- [2] Néel L 1948 *Ann. Phys.* **3** 137
- [3] Mahajan A V, Johnston D C, Torgeson D R and Borsa F 1992 *Phys. Rev. B* **46** 10966
- [4] Claus H and Veal B W 1997 *Phys. Rev. B* **56** 872
- [5] Snyder G J, Booth C H, Bridges F, Hiskes R, DiCarolis S, Beasley M R and Geballe T H 1997 *Phys. Rev. B* **55** 6453
- [6] Yoshii K and Nakamura A 2000 *J. Solid. State Chem.* **155** 447
- [7] Yoshii K 2001 *J. Solid. State Chem.* **159** 204
- [8] Andrzejewski B, Kowalczyk A, Frackowiak J E, Tolinski T, Szlaferek A, Pal S and Simon Ch 2006 *Phys. Status Solidi b* **243** 295
- [9] Avisou A, Dufour C, Dumesnil K, Rogalev A, Wilhelm F and Snoeck E 2008 *J. Phys.: Condens. Matter* **20** 265001
- [10] Nguyen H C and Goodenough J B 1995 *Phys. Rev. B* **52** 324
- [11] Azad A K, Mellergard A, Eriksson S G, Ivanov S A, Yunus S M, Lindberg F, Svensson G and Mathieu R 2005 *Mater. Res. Bull.* **40** 1633
- [12] Rodriguez-Carvajal J 2001 *An Introduction to the Program FullProf 2000* Laboratoire Léon Brillouin, CEA-CNRS, Saclay
- [13] Belayachi A, Nogues M, Dormann J L and Taibi M 1996 *Eur. J. Solid State Inorg. Chem.* **33** 1039
- [14] Kanamori J 1959 *J. Phys. Chem. Solids* **10** 87
- [15] Pickett W E 1998 *Phys. Rev. B* **57** 10613
- [16] Miura K and Terakura K 2001 *Phys. Rev. B* **63** 104402
- [17] Ueda K, Tabata H and Kawai T 1998 *Science* **280** 1064
- [18] Treves D 1962 *Phys. Rev.* **125** 1843
- [19] Tseggai M, Nordblad P, Tellgren R, Rundlöf H, André G and Bourée F 2008 *J. Alloys Compounds* **457** 532
- [20] Tamine M, Nogues M, Dormann J L and Grenèche J M 1995 *J. Magn. Magn. Mater.* **140–144** 1765